

氏 名	Servomaa Henri Tuomas
生 年 月 日	
本 籍	フィンランド
学 位 の 種 類	博士（工学）
学 位 記 番 号	博乙第 258 号
学位授与の日付	2002 年 9 月 30 日
学位授与の要件	論文博士（学位規則第 4 条第 2 項）
学位授与の題目	Determination of snowfall characteristics from image, microwave and optical data（画像処理，レーダ，ライダーによる降雪特性観測）
論文審査委員（主査）	村本健一郎（工学部・教授）
論文審査委員（副査）	長野 勇（研究科・教授） 橋本 秀雄（工学部・教授） 八木谷 聡（研究科・助教授） 松浦 弘毅（工学部・教授）

学 位 論 文 要 旨

Abstract

In this study, a new, comprehensive and automatic snowfall observation system was built, and techniques that could be used in the estimation of snowfall characteristics were developed. The instruments used include two microwave radars, a lidar, a CCD camera based imaging system and high accuracy electrical balances for reference data. A special emphasis has been on obtaining good temporal resolution, which has been often sacrificed in favor of better prediction accuracy of snowfall rate. The measurements were also contained in a small area to be sure that all instruments record data from the same target. One radar and the lidar recorded an atmospheric profile up to 6000 m, while the other radar, the imaging system and the balances recorded snowfall on the ground level. The combination of optical, microwave and direct visual observations of snowfall show that a change in cloud conditions can result in snowfall having different characteristics. The lidar backscatter was used as main indicator of transitions in cloud conditions. A direct visual evaluation of snowflake size distribution using a CCD-camera shows that it is extremely helpful in order to interpret radar data. The velocity distribution measured using video camera showed no large variations between snowfall events. However, the results suggest that it could be useful in detecting graupel and hail.

1 Background

Snowfall plays an important part in fields related to radio wave attenuation and propagation. It is not only important in considerations relating to meteorology and the physics of precipitation, but also for various engineering applications such as remote sensing and telecommunications and lately in global climate monitoring research. Generally, all radio communications are affected by the atmosphere, and depending on the frequency, rain and snowfall have large scattering properties. This is the basis for the monitoring of different atmospheric events using both active and passive instruments at different electro-magnetic wavelengths, ranging from meters to micrometers and up to the visible spectrum.

Because of its good sensitivity and broad range, the weather radar is one of the main instruments used in the study of snowfall. It was first shown by Marshall and Gunn that the radar reflectivity factor Z is related to snowfall rate R by the so-called $Z - R$ relation which is written as

$$Z = BR^{\beta} \quad [mm^6/m^3] \quad (1)$$

where Z is reflectivity, R is snowfall rate in mm/h (liquid water) and B and β are coefficients. The relation between the backscattered radar power and reflectivity is usually expressed by a simplified meteorologic radar equation as

$$\overline{P_r} = CL^2 \frac{Z}{r^2} \quad [W] \quad (2)$$

where $\overline{P_r}$ is the average received power, C includes constant radar and target dielectric parameters, r is the distance from the target scatterers and L is the path loss.

Also, the flake size distribution can be approximated by a negative exponential function.

$$R = \frac{\pi}{6} \sum_i \rho_{i,snow} v_i N_i D_i^3 \quad [mm/h] \quad (3)$$

where N_i is the number of flakes having diameter D_i and $\rho_{i,snow}$ is the density of the corresponding flake and v_i its falling velocity. The radar reflectivity, assuming Rayleigh scattering and discrete data, is then given by

$$Z = \sum_i N_i D_i^6 \quad [mm^6/m^3] \quad (4)$$

where N_i is, again, the number of flakes having diameter D_i .

The above models have been subjected to long research and are now rather established in this field. However, the various empirically determined coefficients in the models tend to differ rather largely by season, location, meteorological conditions and so forth. Although the prediction accuracy of the $Z - R$ relation can be very good (coeff. of determination R^2 typically ≥ 0.8), this is usually achieved at a great sacrifice in temporal and spatial resolution.

The main physical parameters involved in radar observations of precipitation are: particle size distribution (SD), velocity distribution (VD) and in cases other than rain, the particle density. These parameters are difficult to determine accurately using a radar, therefore, in this study, direct observation of the falling particles is done by CCD camera.

2 Instruments

The instruments include 2 small weather radars, an optical lidar, an imaging device using a CCD video camera and 2 high-sensitivity electric balances. Data from a mobile weather station is also used to monitor general meteorological conditions. All data is recorded at short time intervals by computers that have their clocks synchronized to a common time (UT) reference. Furthermore, observations - including reference - are spatially contained in a small area. Therefore, errors due to distances between instruments and target can be neglected. Results from snowfall observations made in Kanazawa in January and February 2000 are presented. This city, by the Japan sea coast, is peculiar in that it experiences rather heavy snowfalls despite being located at a low latitude (approx. $36^\circ 20'N$).

Most of the instruments have been integrated into an automatic framework, as outlined in Fig. 1. The instruments are all located within an area of 30 by 30 meters. A total of 3 workstations are needed to operate and record measurement data via serial RS232C interfaces. The clocks of each computer on the network are synchronized using NTP (Network Time Protocol), with a GPS signal as reference on the time server. One workstation is set a part for backups and lastly, a shared database has been built on another workstation. Since clocks are synchronized with respect to network time, a reliable time reference is recorded with all measurements, a crucial point for obtaining small temporal resolution and reliable comparisons between datasets.

Table 1 summarizes the specifications for the radars and the lidar. The radars are known as

Table 1: Radar and ceilometer specifications.

	POSS	MRR	Ceilometer
Maker/model	Andrew	METEK	Vaisala CT25K
λ	2.85 cm	1.25 cm	905 nm
Power	43 mW	50 mW	8.9 mW ave
Operation	FM-CW	FM-CW	Pulse
Integr. time	1 min.	1 min.	30 sec.
Vert. res.	NA	200m	30m
Meas. angle	20°	zenith	9°
Meas. height	ground level	6000m	7000m

POSS and MRR, which stand for Precipitation Occurrence Sensor System and Micro Rain Radar, respectively. The POSS is a small C-band bistatic radar with a small sensing volume (approx. 1 m^3) very near the transmitter and receiver. The MRR is a conventional monostatic X-band vertical pointing radar. The optical lidar, called ceilometer, operates in the near infra-red spectrum. It is similar in operation to the vertical radar, except that RF components are replaced by optical ones.

3 Results

Data recorded during 6 days in January and February 2000 was analyzed, comprising a total of 104 hours of snowfall. These were divided 90 snowfall events using the following algorithm: if the integrated ceilometer backscatter up to 90 m (3 cells) is larger than $50 (10000 \text{ srad})^{-1}$ (determined experimentally) and the balance data indicates a rate above 0.3 mm/h , then we conclude that it is snowing. If either criteria is not met, then there is no precipitation and a probable change in cloud condition occurs.

The $Z - R$ relation coefficients B and β , along with SD and VD parameters were calculated for all the events and plotted on the $B - \beta$ plane. An example of the event locations on this plane are shown in Fig. 2 for Feb. 17.

It can be noticed that all values are located left of the grey line and there is large overall variation of both B and β values. However, the values of β tend to gather near the $\beta = 1$ line. These points also form 2 clusters around $B=400$ and $B=900$. The clusters are differentiated by SD characteristics, while points located well above or lower the $\beta = 1$ line are not well differentiated using the SD parameters. It is likely that they are cases of very mixed snowfall, with possibly hail or rain content.

4 Conclusions

The SD parameters N_0 , λ and mean diameters were calculated for all events and plotted in the $B - \beta$ plane. It could be observed that two clusters having very similar β values, but differing largely in values of B were formed.

The main goals of the observation system, namely, fine temporal resolution and good synchronization of simultaneous measurements using multiple instruments were achieved. Atmospheric profiling was done using a vertical radar and an optical lidar, while ground level measurements were done with a small bistatic radar and an imaging system. Two electric balances provided reference snowfall rate data. The coefficient of determination values R^2 for the established $Z - R$ relations were from 0.306 to 0.959 with only 2 events being under 0.572. This is an encouraging result when keeping in mind that temporal resolution was 1 minute. The average value for B was 630 and for 1.08 for β . These are very near the values of $B = 427 - 554$ and $\beta = 0.88 - 1.09$ reported by for observations made in Hokkaido, northern Japan.

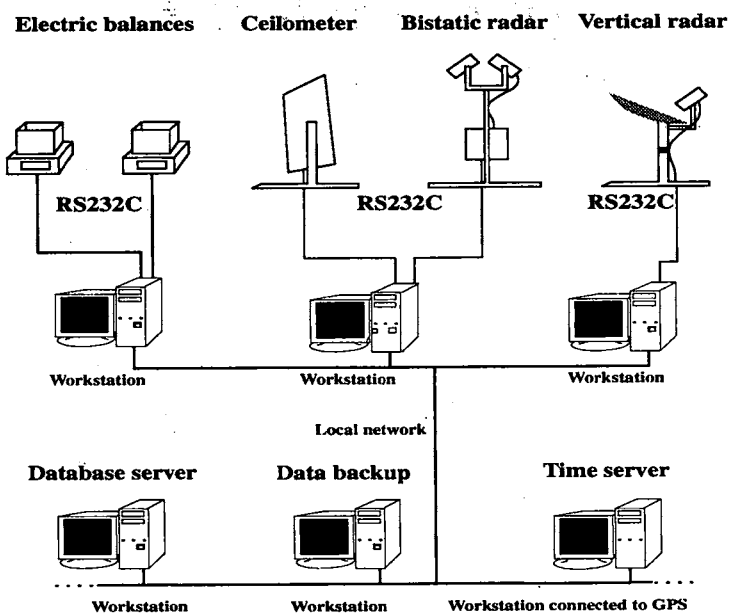


Figure 1: Diagram of the continuous monitoring equipment.

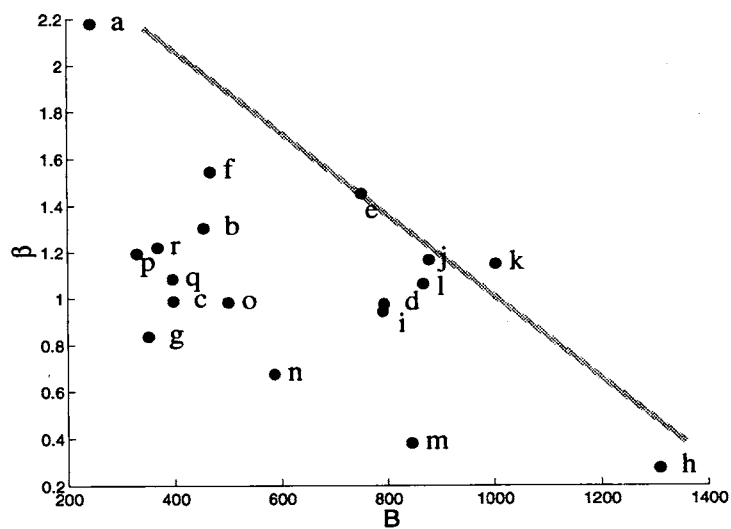


Figure 2: Snowfall events on the B - β plane.

学位論文審査結果の要旨

平成 14 年 7 月 30 日の第 1 回学位論文審査委員会、および同 8 月 1 日の口頭発表と第 2 回学位論文審査委員会において審査した結果、以下の通り判定した。

降雨や降雪は社会的に大きな影響を及ぼすので、その予測は重要である。降雨や降雪の短期予測には、レーダがよく用いられる。降雨に関してはレーダの反射特性が解析されているが、降雪に関しては降雪粒子の誘電率・形状因子など多くの因子が複雑に関係しているため、粒子とレーダ反射因子との対応は詳細には解明されていなかった。

本論文では、降雪粒子とレーダ反射因子との関係を解明することを目的とした。まず最初に、小型レーダ、ライダー、画像処理装置ならびに降雪強度計を近接・連動させた統合型降雪観測システムを開発し、同一観測空間に対して、これらの機器による同期自動観測の可能なシステムを構築した。次に、このシステムを用いて降雪のレーダ反応因子 Z と降雪強度 R の短時間間隔測定から、高精度の Z - R 関係を求め、粒子の物理的特徴量（粒径分布等）が Z - R 関係に及ぼす影響を明かにした。更に、ライダーによる粒子の光学的計測から、上空の雲との関係も調べた。

以上の研究成果は、降雪粒子とレーダ反射因子との関係を定量的に解明しており、その学術的価値が高く、また、気象レーダや衛星を用いた降雪の発生機構の解明や降雪予測へも応用でき、本論文は博士（工学）論文に値するものと判定する。